A FUEL CELL MODEL FOR BUILDING COGENERATION APPLICATIONS

Alex Ferguson V Ismet Ugursal
Canadian Residential Energy End-use Data and Analysis Centre
Halifax, Nova Scotia, Canada B3J 1B6
fergusoa@is2.dal.ca ismet.ugursal@dal.ca

ABSTRACT

A quasi steady state model for cogeneration PEM fuel cell systems has been developed for use in integrated building simulation. The model can predict the fuel cell system fuel use, and heat and electricity production in response to building loads. The model, including theory, structure and validation is discussed, and preliminary results demonstrating the model's use with a building simulation program are presented.

INTRODUCTION

Various fuel cell systems are being developed to replace the conventional internal combustion engine in automotive applications because they can achieve a higher theoretical efficiency than a comparable Carnot cycle and produce substantially fewer emissions. Fuel cells offer a potential for highly efficient electrical generation with reduced emissions, and show promise for stationary cogeneration applications in residential, commercial and institutional buildings. While the operational efficiency of a fuel cell power plant increases as a function the plant's design output, fuel cells have demonstrated superior performance than comparable combustion plants at rated electrical generation capacities from 5 kW to 2 MW [9], a range that includes the energy requirements of most buildings.

Stationary power fuel cells typically burn natural gas, and release fewer environmentally harmful emissions than those produced by a combustion cogeneration plant. With a fuel cell, carbon dioxide emissions may be reduced by up to 49%, nitrogen oxide (NO_X) emissions by 91%, carbon monoxide by 68%, and volatile organic compounds by 93% [5]. In Canada, natural gas is a widely available, accepted, reliable and cost effective alternative to fuel oil for space and domestic hot water heating applications, and is the fuel of choice of electrical utilities. Once commercially available, it is anticipated that an efficient natural gas fuel cell will offer an economical alternative to both combustion cogeneration plants and centralized power generation.

Four natural gas fuel cell technologies have matured to the point where they are suitable for use in stationary cogeneration applications: Phosphorous Acid Fuel Cells (PAFC), Proton Exchange Membrane Fuel Cells (PEM), Solid Oxide Fuel Cells (SOFC), and Molten Carbonate Fuel Cells (MCFC). So far, manufacturers have focused on PAFC and PEM cells for use in cogeneration applications, but newer SOFC and MCFC technologies offer higher efficiencies and are receiving increasing attention.

As fuel cell technologies may see widespread public use in the near future, there exists a need for a modelling tool able to accurately predict a fuel cell system's behavior as it responds to conditions in the building. Such a tool would be useful in:

- estimating fuel cell system energy production and fuel use in static cogeneration applications,
- determining the suitability of fuel cell systems in different climates and building types,
- determining the optimal size of a fuel cell system for a given application, and
- evaluating different system optimization and control strategies for fuel cell systems.

The present article discusses a quasi steady state PEM fuel cell component model developed for use with the building simulation program ESP-r[1]. The model can predict the fuel cell system fuel use, and electrical and thermal energy production in response to building loads. No attempt was made to optimize the fuel cell system operation or configuration (eg. inclusion of heat or electrical storage devices). It is anticipated that further studies using the model will address these issues.

PEM FUEL CELL SYSTEMS

A fuel cell is a device that converts chemical energy directly into electrical energy. This conversion is facilitated by an electrode-electrolyte structure that operates on principles similar to chemical batteries. However, while a battery's fuel and oxidant supplies are stored within the cell, fuel cells permit fuel and oxidants to continuously flow through the cell. This is advantageous, because a fuel cell need not be taken off-line to be refuelled.

While many fuels may react with oxygen to produce electricity directly, hydrogen has the highest electrochemical potential and yields the highest theoretical fuel conversion

[1]Energy Systems Research Unit (ESRU)
University of Strathclyde
http://www.esru.strath.ac.uk/

efficiency (η = 93% at 298 K) [7]. Thus, hydrogen is typically used to fuel low temperature PEM fuel cells. Since natural sources of hydrogen are not available, it must be obtained from a hydrocarbon fuel such as natural gas.

PEM Fuel cell systems consist of several sub-systems. These include the fuel cell stack, the fuel processor, and auxiliary systems required for operation.

Fuel Cell Stack

The fuel cell stack is the electrode-electrolyte structure where energy conversion occurs. The electrode in contact with the fuel stream is called the anode, while the electrode in contact with the oxidant is termed the cathode. In PEM fuel cell systems, the stack typically operates at 80 °C [3]. The reactions occurring in the PEM fuel cell stack proceed as follows:

$$Anode: \quad H_2 \rightarrow 2H^+ + 2e^- \tag{1}$$

$$Cathode: \quad 2H^+ + \frac{1}{2}O_2 + 2e^- \rightarrow H_2O \tag{2}$$

$$Overall: \quad H_2 + \frac{1}{2}O_2 \rightarrow H_2O \tag{3}$$

The theoretical maximum amount of electrical energy that can be obtained from the electrochemical reactions occurring in the fuel cell stack is equal to the change in the Gibbs free energy within the cell [6]. The total amount of energy released in the electrochemical reactions is equal to the enthalpy change within the cell. Thus, the theoretical maximum efficiency of conversion from chemical to electrical energy, η_{max}, is obtained as the ratio between the change in the Gibbs free energy (ΔG_{stack}) and the change in the enthalpy (ΔH_{stack}) that occur in the cell stack:

$$\eta_{max} = \frac{\Delta G_{stack}}{\Delta H_{stack}} \tag{4}$$

The Second Law of Thermodynamics requires that the theoretical maximum efficiency be achieved only when the cell operates under reversible conditions, and these conditions are approached when there is no electrical load on the stack. Inefficiencies associated with the reactions, called polarization losses, lower the overall cell efficiency under loaded conditions. Three types of polarization losses exist:

- activation polarizations that result from the electrochemical barriers that oppose current and ion flow,
- concentration polarizations that result from local depletion of the reactants on the electrodes, and
- ohmic polarizations that result from electrical resistances within the cell.

A representative polarization curve is depicted in Figure 1. Activation polarization losses increase rapidly as the stack load increases from zero but then quickly approach a constant value. Conversely, concentration polarization losses are only significant under high current loadings. In

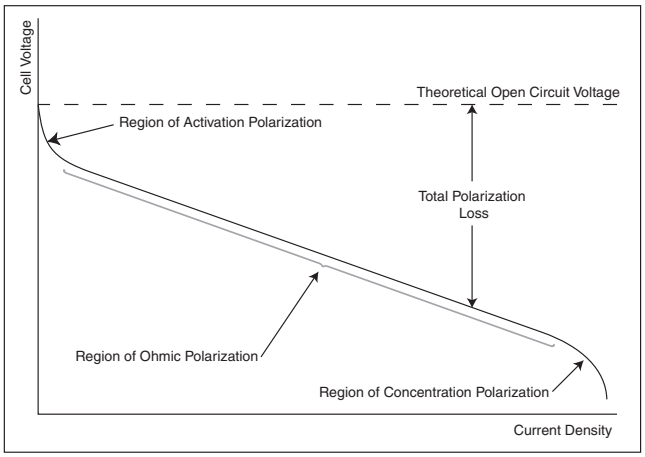

Figure 1: Typical fuel cell polarization curve

the region where the activation polarization losses are effectively constant and concentration polarization losses are effectively insignificant, the shape of the polarization curve is only dependent on the ohmic polarization losses. Since ohmic losses area linear function of the current, the cell voltage polarization curve displays linear behavior though this region, called the Tafel region. The voltage-current characteristics of real fuel cell systems do not deviate from the linear behavior of the Tafel region, as the activation and polarization regions are not normally suitable for fuel cell operation [1].

Fuel Processor

The fuel processor is used to convert a hydrocarbon fuel, such as methane, into a stream containing hydrogen that may be oxidized in the fuel cell stack. In this process, called reforming, hydrocarbons are reacted with high temperature water vapor.

The fuel processor typically incorporates four separate reaction vessels [3]:

Reformer: The hydrocarbon and steam streams first pass through a high temperature reactor vessel, called a reformer, where most of the fuel is converted into a mixture of hydrogen and carbon monoxide. Some of the carbon monoxide produced in the reformer may also react with water to form carbon dioxide. The reformer operating temperature is dependent on the fuel used, and may range from 250 °C (methanol) to over 700 °C (methane).

High Temperature Water Shift Reactor: The high temperature water shift reactor (HTWS) is used to convert carbon monoxide to carbon dioxide. The HTWS reactor typically operates at temperatures between 260-320 °C.

Low Temperature Water Shift Reactor: The low temperature water shift (LTWS) reactor is used to convert the remaining carbon monoxide to carbon dioxide. The

LTWS reactor typically operates at temperatures between 200-260 $^{\circ}$C.

Preferential Oxidation Reactor (PROX): PEM fuel cells use a preferential oxidation (PROX) reactor to shift any remaining carbon monoxide to carbon dioxide by introducing a suitable amount of oxygen to the reformate stream. This is done because trace amounts of carbon monoxide (larger than 10 parts-per-million) will be absorbed on the platinum catalyst and block access of hydrogen to the catalyst sites, reducing the performance of the cell.

Four separate reactions occur in the fuel processor:

$$C_xH_yO_z + (x-z)H_2O \leftrightarrow xCO + (x + \frac{y}{2} - z)H_2 \quad (5)$$

$$CO + H_2O \leftrightarrow CO_2 + H_2 \quad (6)$$

$$CO + 0.5O_2 \leftrightarrow CO_2 \quad (7)$$

$$H_2 + 0.5O_2 \leftrightarrow H_2O \quad (8)$$

The first reaction (Equation 5) involves the direct conversion of a hydrocarbon fuel ($C_xH_yO_z$) into a mixture of hydrogen and carbon monoxide, and occurs exclusively in the reformer. Equation 6 describes a shift reaction in which carbon monoxide produced in the reformer is reacted with water vapor to produce additional hydrogen and carbon dioxide. This shift reaction is exothermic and occurs in the reformer, HTWS and LTWS reaction vessels. The third and fourth reactions (Equations 7 and 8) occur exclusively in the PROX reactor vessel, where remaining carbon monoxide is converted to carbon dioxide by means of a reaction with oxygen (Equation 7). Oxygen that enters the PROX reactor and does not oxidize with carbon monoxide will react with hydrogen to form water vapor (Equation 8).

Auxiliary Systems

A building cogeneration fuel cell system also incorporates several auxiliary devices required for operation:

Power conditioning unit: The power conditioning unit is used to convert the direct current output from the fuel cell to alternating current suitable for use by building equipment.

Hydrogen burner: The hydrogen burner is used to oxidize any hydrogen not reacted in the fuel cell stack. This prevents the release of combustible gasses to the atmosphere, and also produces thermal energy that may be used for process heating in the fuel processor.

Auxiliary burner: The auxiliary burner is used to provide supplementary heat to the fuel processor for process heating if sufficient thermal energy cannot be recovered from hot process streams.

Heat extraction equipment: During operation, the fuel cell produces heat that must be extracted to ensure that the stack remains at the optimal temperature. This may be done with a water loop that extracts heat for space heating and domestic hot water (DHW) purposes, and a mechanical cooling arrangement that provides cooling during periods of insufficient space heating and DHW demand.

Compressors and pumps: Some PEM fuel cell systems operate at pressures several times that of the ambient, necessitating compressors and pumps.

Heat Recovery: The arrangement of reactors in the fuel processor requires that the reactant streams be heated and then subsequently cooled. This is accomplished by a network of heat exchangers that transfers heat from streams requiring cooling to streams requiring heating.

PEM FUEL CELL MODEL

The probable users of the fuel cell component model are not likely to have a comprehensive electrochemical background. There are many comprehensive first-principle models in the literature, but a review of these models indicated that substantial user knowledge is required for their effective use, and that they often provide detailed treatment of aspects of the fuel cell that have little significance in building energy modelling. An empirical modelling approach was also considered, but little data have been published on the part load characteristics of fuel cell systems. Thus, to best meet the needs of the identified users, it was decided to adopt a parametric modelling approach.

Electrochemical Model

Recently, Thorstensen published a simplified parametric modelling study of part load system efficiencies for various fuel cell systems [8]. Thorstensen demonstrated that, if the activation and concentration polarizations are ignored, the polarization curve may be represented as a single linear function with the maximum cell potential at zero current (open circuit conditions), and the maximum current occurring at zero cell potential (short circuit conditions). Using this idealized relationship allows a simple relationship describing the efficiency of the electrochemical energy conversion as a function of the power loading to be obtained:

$$\eta_{cell} = \eta_{max}\left(\frac{1+\sqrt{1-\frac{P}{P_{max}}}}{2}\right) \quad (9)$$

where η_{cell} is the electrochemical efficiency of the cell, P is the power loading, and P_{max} is the theoretical maximum power loading.

The idealized linear voltage-current characteristic used by Thorstensen ignores the activation polarization losses that occur in cell operation, and thus over-predicts the cell efficiency. Thorstensen accounts for this discrepancy by using coefficients to fit model results to experimental data. However, a lack of published data on the part-load operation of fuel cell systems makes this approach difficult.

Data obtained from experimental fuel cell stacks indicates that activation polarizations remain effectively constant over

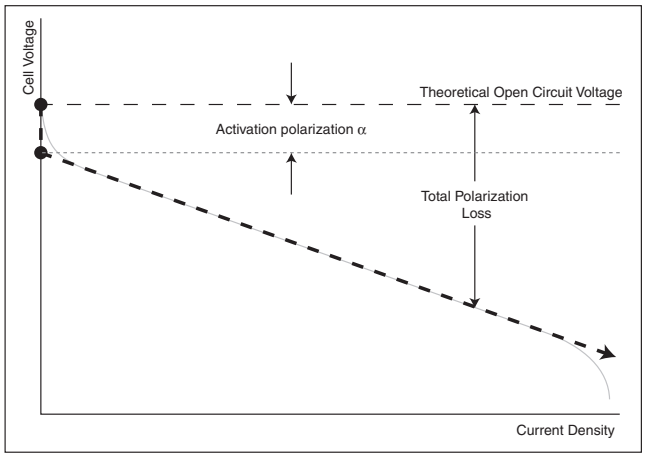

Figure 2: Simplified fuel cell polarization curve

the fuel cell's operating range [1]. If they are assumed to be constant, the activation polarizations may also be considered in the part load efficiency calculation. This is accomplished by introducing a parameter, α, that describes the ratio between the constant activation polarization and the theoretical open cell voltage. The introduction of α permits modification of Thorstensen's model to use two linear line segments instead of one to approximate the fuel cell polarization curve:

- The first segment is a vertical line starting at the cell open circuit reversible voltage and ending at some point on the vertical axis, and
- the second segment is a diagonal line collinear with the Tafel portion of the polarization curve that starts at the endpoint of the first segment.

The approximated polarization curve is depicted in Figure 2. The length of the vertical line segment is determined by the amount α, which is the constant approximation of the activation polarization at full load. Using a method similar to that presented by Thorstensen [8], it is possible to obtain an expression for the part load efficiency as a function of the cell power output. The cell voltage, V, may be expressed as the product of the open cell potential, V_{rev}, and the part load efficiency η_v:

$$V = \eta_v V_{rev} \tag{10}$$

The linear relationship between voltage and current implies:

$$I = I_{sc}\left(\frac{(1-\alpha)-\eta_v}{1-\alpha}\right) \tag{11}$$

where I is the loaded cell current, I_{sc} is the short circuit current, and a is the parameter describing the constant polarization loss. Since the cell output power is the product of voltage and current, Equations 10 and 11 may be combined to obtain the cell power as a function of the part-load efficiency ($P(\eta_v)$):

$$P(\eta_v) = V_{rev} I_{sc} \eta_v \left(\frac{(1-\alpha)-\eta_v}{1-\alpha}\right) \tag{12}$$

The maximum theoretical power can be determined by first differentiating Equation 12 with respect to the part load efficiency (η_v) to obtain Equations 13 and 14.

$$P'(\eta_v) = \frac{d}{d\eta_v} P(\eta_v) \tag{13}$$

$$= V_{rev} I_{sc}((1-\alpha) - 2\eta_v) \tag{14}$$

Then Equation 14 is set equal to zero and the efficiency at the maximum theoretical power is determined:

$$\eta_{v_{P_{max}}} = \frac{1-\alpha}{2} \tag{15}$$

where $\eta_{v_{P_{max}}}$ is the cell part-load efficiency at maximum theoretical power. Maximum power (P_{max}) is obtained by substituting Equation 15 into Equation 12.

$$P_{max} = \frac{V_{rev} I_{sc}(1-\alpha)}{4} \tag{16}$$

Part-load power and part-load efficiency are calculated by substituting Equation 16 into 12:

$$P = 4P_{max}\left(\frac{\eta_v(1-\alpha) - \eta_v^2}{(1-\alpha)^2}\right) \tag{17}$$

$$\eta_v = (1-\alpha)\left(\frac{1+\sqrt{1-\frac{P}{P_{max}}}}{2}\right) \tag{18}$$

The major difference between the two line segment approximation of the polarization curve and the single line segment approximation used by Thorstensen is the consideration of activation polarization. As indicated by Equation 18 this results in scaling the calculated part-load efficiency by the amount $(1-\alpha)$, and ensures that the idealized linear polarization curve approaches an open circuit voltage amount that is less than the reversible voltage. As a result, the model under-predicts the cell voltage through the region of activation polarization, but more accurately predicts the cell voltage through the Tafel region.

Determination of the maximum theoretical power (P_{max}) is another difficulty in the Thorstensen model; this value may differ from both the nominal rated output and the maximum permissible instantaneous output. Thorstensen suggests that this value typically varies from 130% to 180% of the nominal rated output, and the actual value for a given fuel cell system may be difficult to determine from the published literature.

The electrochemical efficiency under full (rated) load is more commonly available in the literature, and may alternatively be used to determine the theoretical maximum power:

$$\eta_{v\,nom} = \frac{\eta_{cell_{nom}}}{\eta_{max}} \tag{19}$$

$$P_{max} = \left(\frac{(1-\alpha)^2}{4(\eta_{v\,nom}(1-\alpha) - \eta_{v\,nom}^2)}\right) P_{nom} \tag{20}$$

where $\eta_{cell_{nom}}$ is the fuel cell stack efficiency at the nominal rated power, and P_{nom} is the cell nominal rated power. Once the cell part load efficiency has been determined, it may be combined to with the maximum theoretical efficiency to obtain the cell conversion efficiency:

$$\eta_{cell} = \eta_v \eta_{max} \tag{21}$$

The gross electrical output of the call can also be determined:

$$\dot{W}_{gross} = \eta_{cell}\eta_{pc}\Delta\dot{H}_{stack} \quad (22)$$

where $\dot{W}_{gross}$,, is the gross alternating current electrical output of the fuel cell, η_{pc} is the nominal efficiency of the power conditioning equipment, and $\Delta\dot{H}_{stack}$ describes the total enthalpy change within the stack.

As not all of the chemical energy released in the fuel cell stack is converted to electrical work, heat is also produced in the stack. This amount of heat, $\dot{Q}_{stack}$, can be determined using the maximum and part-load cell stack efficiencies:

$$\dot{Q}_{stack} = \Delta H_{stack}(1 - \eta_{cell}) \quad (23)$$

To ensure that the fuel cell operates at its optimal temperature, this heat must be extracted from the stack using a heat recovery arrangement or evaporative cooling equipment.

Thermal Model

Each reactor in the fuel cell system is modelled as single control volume with corresponding energy and mass flows:

$$\sum \dot{N}_{k_o} h_{k_o} - \sum \dot{N}_{k_i} h_{k_i} = \dot{Q}_i - \dot{W}_o \quad (24)$$

where $\dot{N}_{k_o}$, is the molar flow rate of species k leaving the control volume, h_{k_o}, is the enthalpy of species k leaving the control volume, $\dot{N}_{k_i}$, is the molar flow rate of species k entering the control volume, and h_{k_i}, is the enthalpy of species k entering the control volume. $\dot{Q}_i$ is the rate at which heat enters the control volume, and $\dot{W}_o$ is the rate at which work is extracted from the control volume.

A review of several conceptual and operating fuel cell system schematics [1, 2, 3] indicated that the required heating and cooling can be accomplished with different arrangements of heat exchangers and fluid paths. A model that explicitly simulated one of these arrangements might be less accurate when other fuel cell systems are considered, and the inherent complication associated with the heat exchanger network model may prevent users from modifying the model to better represent the system at hand. To preserve the flexibility of the fuel cell model, an alternative process modelling technique known as pinch analysis [4] is used to determine the magnitude of the heat recovered in the fuel cell system equipment. Pinch analysis computes the maximum amount of thermal energy that may be transferred between the hot and cold streams regardless of the arrangement used to accomplish the heat transfer. Consequently, a model based on pinch analysis is sufficiently generic to model different fuel cell systems without requiring modification. However, it should be noted that the magnitude of heat recovery predicted using pinch analysis represents the theoretical upper limit for heat recovery, and the actual amount of heat recovery accomplished in a heat recovery network will be lower than the theoretical upper limit.

In pinch analysis, all of the processes requiring heating are represented with a single composite temperature-enthalpy curve that depicts the the total system heating requirement

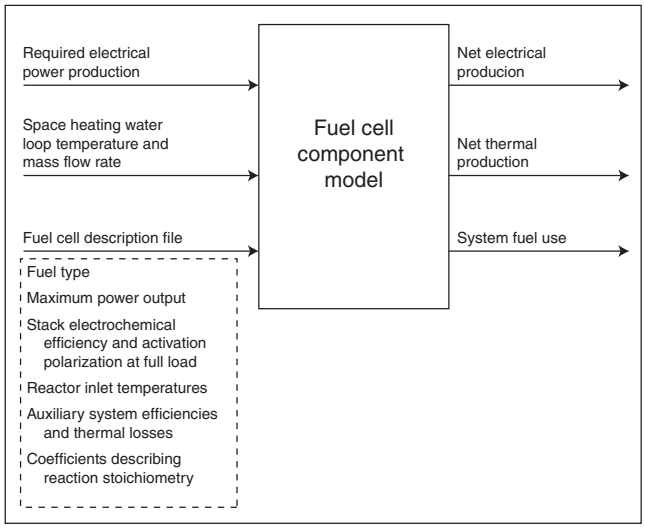

Figure 3: Inputs to and outputs from the fuel cell component model.

at each temperature. Similarly, all of the processes requiring cooling and hot exhaust streams undergoing heat recovery are represented with a single composite curve that depicts the total system cooling requirement at each temperature. Since enthalpy is a relative measure, it is possible to place the two composite curves on a single temperature-enthalpy plot. The composite curves may be shifted to ensure that the minimum temperature difference is maintained throughout the process temperature range. Thus, using the pinch analysis method, it is possible to determine the theoretical upper limit for heat recovery between a series of processes requiring heating and a series of streams that require cooling. Also, the need for external utility heating and utility cooling may be determined.

Since the user is able to adjust the minimum temperature difference used in the thermal model based on pinch analysis, the thermal model can be modified to reflect the less than ideal performance of an actual heat recovery system compared to that of an ideal one. Future work investigating the error inherent in the use of pinch analysis through comparative testing with explicitly modelled heat recovery arrangements would be helpful to develop guidelines for accurately specifying the minimum temperature difference.

Model Architecture

Data flow into and out of the fuel cell component model is illustrated in Figure 3. The model predicts the fuel cell operating point by performing the following steps:

1. Read inputs (fuel cell system description, required net power production, inlet temperature and mass flow rate of space heating recovery water loop).

2. Determine the molar flow rates of reactants necessary to provide a single mole of hydrogen to the fuel cell

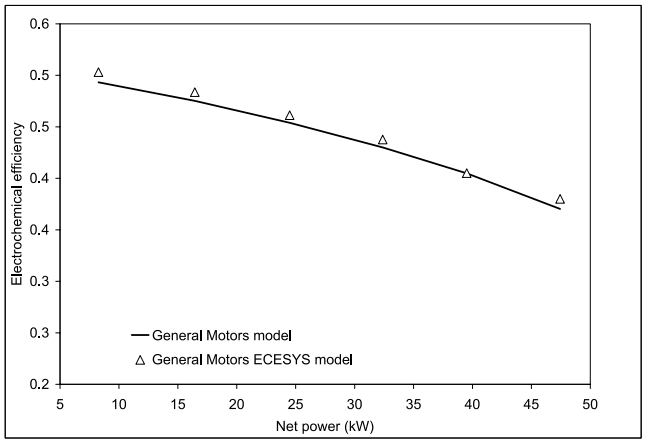

Figure 4: Comparison of fuel cell system efficiency estimates, GM study and fuel cell component model.

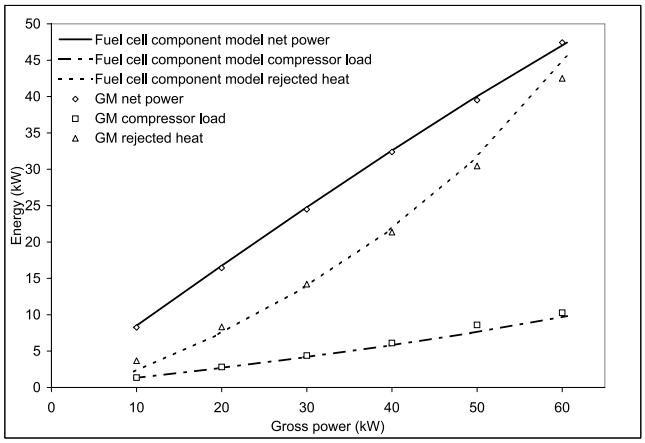

Figure 5: Comparison of fuel cell energy flow fuel predictions, GM study and fuel cell component model

stack by applying a mass balance at each reactor in the fuel cell system.

3. Determine the fuel cell theoretical electrochemical performance under zero electrochemical load (calculate η_{max}).

4. Estimate gross power output and iterate until the calculated net power production and the required net power production are equal:

   (a) Determine stack part load electrochemical efficiency η_v.

   (b) Determine the flow rate at which hydrogen must enter the stack to produce the estimated gross power.

   (c) Calculate actual molar flow rates for all species in the fuel cell system.

   (d) Determine the temperature-enthalpy profiles of the heating and cooling processes and the heat that may be recovered for process use.

   (e) Determine the utility heat and supplementary fuel requirements.

   (f) Determine the utility cooling requirement, the maximum amount of energy that may be transferred from the system into the space heating water loop, and the electrical requirement of the auxiliary cooling system.

   (g) Determine the electrical requirement of the compressors and pumps.

   (h) Calculate the net power produced by the cell, accounting for the electrical consumption of the auxiliary systems and the efficiency of the power conditioning unit.

VALIDATION

In the absence of published PEM fuel cell system experimental data, the accuracy of the fuel cell component model was assessed by comparing its predictions to those obtained in a General Motors study [1] of a similar, methanol-fuelled PEM fuel cell. In the General Motors study, a proprietary steady-state fuel cell model was adapted to represent a methanol-fuelled PEM fuel cell and its auxiliary systems. The part-load electrical efficiency of the system was estimated for a given set of operating conditions.

The fuel cell component model was configured by adjusting the input parameters to accurately represent the use of liquid methanol fuel as a source of hydrogen and to reflect the system arrangement and operating conditions described in the General Motors study. The part-load efficiency results reported in the GM study are depicted along with the results obtained with the fuel cell component model in Figure 4. Figure 5 presents a comparison of the estimated power output, waste heat and compressor loads of the two models. The results agree well.

INTEGRATED BUILDING SIMULATION

Cogeneration fuel cells in wet central heating plants may be modelled using the fuel cell component model and ESP-r's explicit plant modelling facilities. In this arrangement, the fuel cell heat recovery equipment is considered as a massless control volume (node i), with the inlet representing incoming cool water, and the outlet representing outgoing hot water (shown in Figure 6). The fuel cell system may reject heat into the water stream, thereby raising the temperature of the water. By applying the First Law of Thermodynamics to the single node, an expression describing the energy balance in the control volume is obtained (Equation 25):

$$\dot{m}C_p(T_i - T_h) = \dot{Q}_{HR} \tag{25}$$

where $\dot{m}$ is the mass flow rate of the water in the water heating loop, C_p is the specific heat of water, T_h is the temperature of the water entering node i, T_i is the temperature of the water leaving node i, and $\dot{Q}_{HR}$ is the heat that may be recovered from the fuel cell system. The fuel cell component model determines $\dot{Q}_{HR}$ by (1) adding the temperature enthalpy profile of the water heating loop water to the composite temperature-enthalpy curves and (2) adjusting the water and

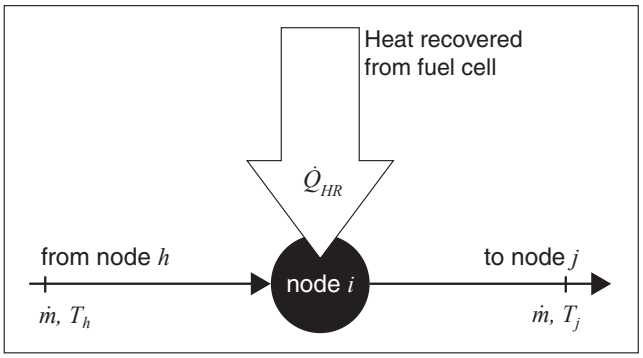

Figure 6: Arrangement of fuel cell component model in wet central heating plant.

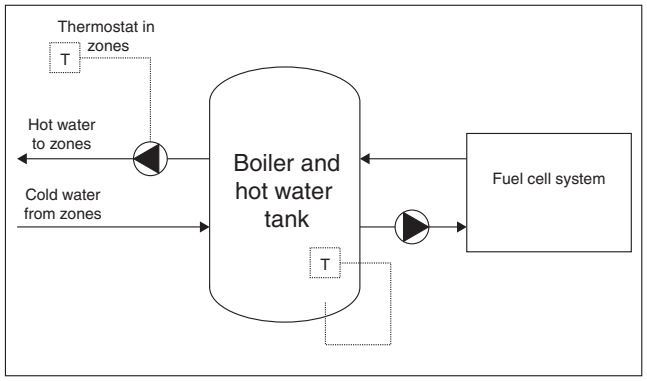

Figure 7: Arrangement of fuel cell component model in wet central heating plant.

exhaust gas outlet temperatures to ensure that a minimum temperature difference exists between the water heating loop and the streams that it exchanges heat with.

PRELIMINARY RESULTS

To demonstrate the use of the fuel cell component model with ESP-r, the model was incorporated into a wet central heating plant model. In this arrangement (depicted in Figure 7), a single, massless node representing the fuel cell component model's heat recovery facilities was connected to a gas fired hot water tank by means of a water loop. The hot water tank was also connected to hot water radiators in the heated space. The plant was connected to a model of a two bedroom house and the simulation was configured to use ESP-r's default climate file[2]. The thermal and electrical load profiles for the house on an arbitrary winter day are depicted in Figure 8. The household thermal demand was determined using ESP-r's simulation facilities while the electrical demand was specified according to an arbitrary, although realistic, schedule. The large electrical demand in the evening hours corresponds to increased electrical consumption by cooking end-uses. The fuel cell was managed using a control loop that matched the electrical output to the building electrical demand, while the circulator providing flow to the zones was controlled by a thermostat in the largest zone. The hot water

[2]Climate data from Jan 1. to Dec 31, 1967, for a location at 52 °N and 0 °E

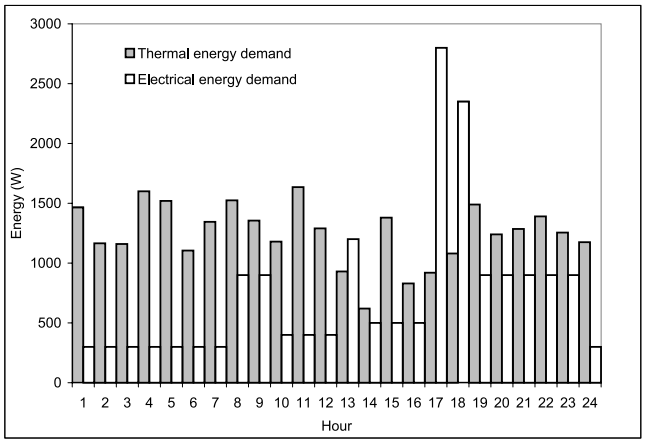

Figure 8: Load profile for a two-bedroom house in a temperate climate on an arbitrary winter day.

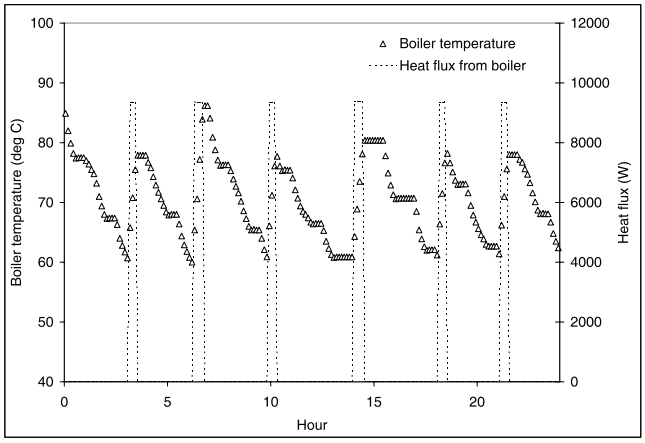

Figure 9: Boiler temperature and plant heat flux for wet heating plant without fuel cell.

tank was controlled using an on-off controller that would activate a 11 kW burner if the tank temperature dropped below 60 °C, and would deactivate the burner if the temperature rose above 80 °C. The circulator providing flow to the fuel cell was set to operate constantly..

The results for two different operating scenarios follow. (Figures 9 to 11). In each case, the boiler storage temperature is plotted over a 24-hour period, along with the heat flux into the boiler control volume from the gas burner and the fuel cell heat recovery equipment. Figure 9 depicts the base scenario where the wet central heating plant operated without a fuel cell system. In this configuration, the burner must supply all of the required heat to the boiler, and can be seen operate periodically throughout the day.

In the first operating scenario, the fuel cell controller managed the fuel cell output to meet the electrical load in the building at each time-step. The results, depicted in Figure 10, show that the fuel cell makes a significant contribution to the plant heat production in the afternoon and evening periods when electrical demand is highest. No heat input

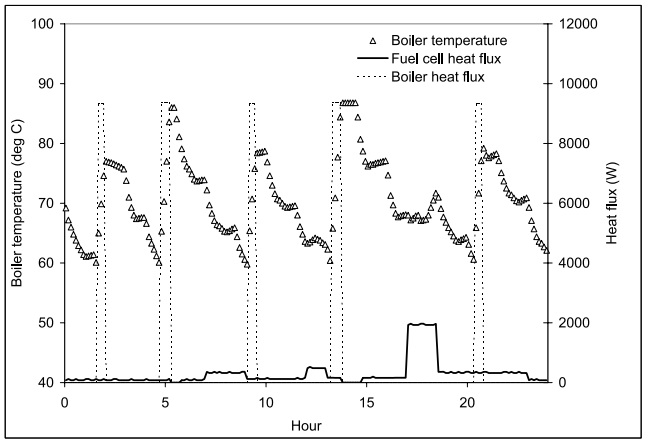

Figure 10: Boiler temperature and plant heat flux for a cogeneration fuel cell system with variable electric output.

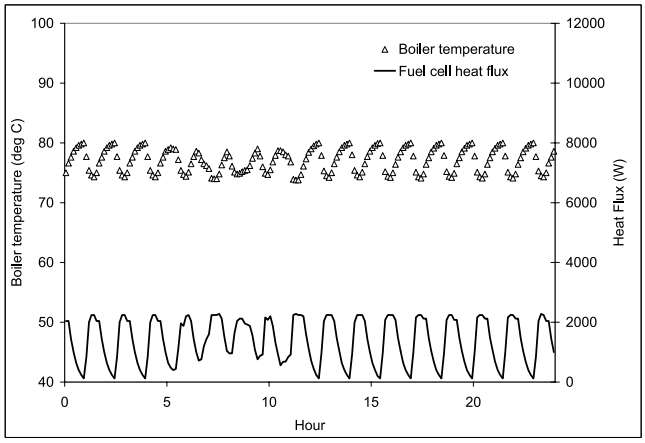

Figure 11: Boiler temperature and plant heat flux for a cogeneration fuel cell system with constant 3kW electric output.

is required from the boiler during these periods. In the second scenario, the fuel cell was configured to operate at a constant output of 3 kW. While this output is considerably higher than the typical residential requirement, it might be representative of an arrangement where the homeowner could sell surplus electricity to the local utility. The results, presented in Figure 11, show that the heat recovered from the fuel cell is sufficient to keep the boiler storage temperature above 70 °C over the entire day without any heat input from the burner.

CONCLUSIONS

A parametric model describing the behavior of static cogeneration fuel cell systems was developed and validated using available published results. Comparative testing of the thermal model with an explicitly modelled fuel cell heat recovery system would strengthen confidence in model results and would help establish guidelines for specifying a minimum approach temperature, which characterizes the thermal performance of the fuel cell system.

The fuel cell component model is suitable for use with integrated building simulation software, and for studying fuel cell system response to building loads in different applications and climates. It is planned to use the fuel cell component model to optimize fuel cell system configurations for residential congeneration systems. Further work will be carried out to develop system sizing guidelines, to optimize control strategies for both thermal and electrical production, and to investigate the benefits of thermal and electrical storage, and fuel cell cogeneration system suitability in different climates.

ACKNOWLEDGMENTS

This project is supported in part by the CAMNET Energy Technology Centre under the Assistance for Academic Research Supporting CETC's Long Term Building-Simulation Research Objectives program. The authors also gratefully acknowledge the contributions lan Beausoleil-Morrison has made to this work and comments offered by anonymous reviewers.

REFERENCES

[1] S. Chalk. Research and Development of Proton-Exchange-Membrane (PEM) fuel cell system of Transportation Applications. Allison Gas Turbine Division, General Motors Corporation, 1996.

[2] D. Doss. Fuel processors for automotive fuel cell systems: a parametric analysis. Journal of Power Sources, (102):1–15, 2001.

[3] J. Hirschenhofer. Fuel Cell Handbook, Forth Edition. Federal Energy Technology Center, US Department of Energy, 1998.

[4] B. Linnhoff. User Guide on Process Integration for the Efficient Use of Energy. Institution of Chemical Engineers, 1994.

[5] D. Scott. Advanced power generation from fuel cells - implications for coal. IEA Coal Research, 1993.

[6] K. Spring. Direct Generation of Electricity. Academic Press, Inc., 1965.

[7] G. Sutton. Direct Energy Conversion. McGraw-Hill, Inc., 1966.

[8] B. Thorstensen. A parametric study of fuel cell system efficiency under part-load operation. Journal of Power Sources, 92:9–16, 2001.

[9] R. Wolk. Fuel cells for homes and hospitals. IEEE Spectrum, pages 45–52, May 1999.